Large-scale sub-100 nm compound plasmonic grating arrays to control the interaction between localized and propagating plasmons

Arash Farhang,[a] Thomas Siegfried,[b] Yasin Ekinci,[b] Hans Sigg,[b] and Olivier J. F. Martin[a]

[a]EPFL-STI-IMT-NAM, Station 11, ELG 239, CH-1015 Lausanne, Switzerland
olivier.martin@epfl.ch
[b]Paul Scherrer Institute, Laboratory for Micro- and Nanotechnology, ODRA/100, 5232 Villigen-PSI, Switzerland

Abstract. Compound plasmonic resonances arise due to the interaction between discrete and continuous metallic nanostructures. Such combined nanostructures provide a versatility and tunability beyond that of most other metallic nanostructures. In order to observe such resonances and their tunability, multiple nanostructure arrays composed of periodic metallic gratings of varying width and an underlying metallic film should be studied. Large-area compound plasmonic structures composed of various Au grating arrays with sub-100 nm features spaced nanometers above an Au film were fabricated using extreme ultraviolet interference lithography. Reflection spectra, via both numerical simulations and experimental measurements over a wide range of incidence angles and excitation wavelengths, show the existence of not only the usual propagating and localized plasmon resonances, but also compound plasmonic resonances. These resonances exhibit not only propagative features, but also a spectral evolution with varying grating width. Additionally, a reduction of the width of the grating elements results in coupling with the localized dipolar resonance of the grating elements and thus plasmon hybridization. This newly acquired perspective on the various interactions present in such a plasmonic system will aid in an increased understanding of the mechanisms at play when designing plasmonic structures composed of both discrete and continuous elements. [DOI: 10.1117/1.JNP.8.083897]

Keywords: compound plasmonics; grating; coupling; hybridization; surface plasmons; thin film.

Paper 13068SS received Aug. 8, 2013; revised manuscript received Nov. 27, 2013; accepted for publication Dec. 5, 2013; published online Jan. 9, 2014.

1 Introduction

Plasmonic systems composed of metallic nanostructures surrounded by a dielectric environment support surface plasmons, i.e., optical resonances bound to the metal-dielectric interface that are based on the excitation of free electrons in the metal.[1–3] In small discrete systems, such as nanospheres, dimers, nanoprisms, and subwavelength gratings, these resonances exhibit a localized response and are commonly referred to as localized surface plasmons (LSPs).[3] In extended systems, such as a continuous film, long metallic strips, or gratings that extend over several wavelengths, they exhibit a delocalized/propagative response and are simply referred to as surface plasmon-polaritons (SPPs).[1,2,4,5]

LSPs have shown to be useful in applications such as trapping,[6,7] cancer treatment,[8–11] surface-enhanced Raman spectroscopy,[12–15] and light harvesting,[16,17] while SPPs have shown great use in applications such as biosensing[18,19] and as optical interconnects in conventional integrated circuits.[20–23] Systems composed of both continuous and discrete structures are of particular interest since they exhibit enhanced optical properties,[24–44] improved light harvesting,[45–50] matching of radiative and nonradiative losses,[51] and additional degrees of freedom for the tuning of their spectral properties.[24–44]

0091-3286/2014/$25.00

The novelty of this paper is the numerical and experimental demonstration of such a system that can also support new compound plasmonic resonances, i.e., resonances exhibiting both a localized and propagative response.[52] The studied interaction between a metallic grating and a continuous film demonstrates the formation of such resonances, where the field not only propagates along the continuous surface of the film, but is also localized around the grating elements. In addition, unlike grating-assisted excitation of SPPs where it is primarily the periodicity that determines the resonance frequency, here the width of grating elements also plays a critical role in determining the resonance frequency, just as is the case for LSPs. Thus, such compound plasmonic nanostructures provide a versatility and tunability beyond what can be achieved by structures that support only propagating or localized plasmon resonances. This fact is demonstrated here through excellent agreement of both numerical and experimental results.

2 Methods

2.1 *Experimental*

The system that is fabricated and investigated consists of a single Au grating layer of period $\Lambda = 250$ nm and height $h = 15$ nm placed at a distance $s = 20$ nm from the surface of a continuous Au film of thickness $t = 25$ nm. The system is illuminated with TM polarized light over a wide range of incidence angles $\theta = 10$ to 74 deg and investigated over a wavelength range of $\lambda = 500$ to 1000 nm.

Float glass coverslips used for the substrate were cleaned in a Piranha bath. A continuous 25 nm Au base-layer was thermally evaporated (99.99% purity, purchased from Balzers, Germany) with a chromium adhesion layer of 1 nm to minimize damping.[53] For the evaporation of the grating layer, a double-layer photoresist mask was exposed, consisting of a 160-nm polymethyl methacrylate (PMMA) film covered by 60 nm hydrogen silsesquioxane (HSQ). Extreme UV interference lithography (EUV-IL)[54] at the Swiss Light Source was used to create line patterns with a period of $\Lambda = 250$ nm over an area of 1×2 mm^2. PMMA was etched in oxygen plasma (30W RIE power with 20 sccm O_2 flow rate) with the HSQ grating as the etch mask. A grating bilayer consisting of 20 nm SiO_2 followed by 15 nm of Au was then deposited via evaporation. A final liftoff of the photoresist mask was done in acetone under gentle sonication.

SEM images of the structures both from above and along an x-z cross-section and a schematic cross-section, Figs. 1(a) to 1(h), show a $\Lambda = 250$ nm periodicity and grating widths

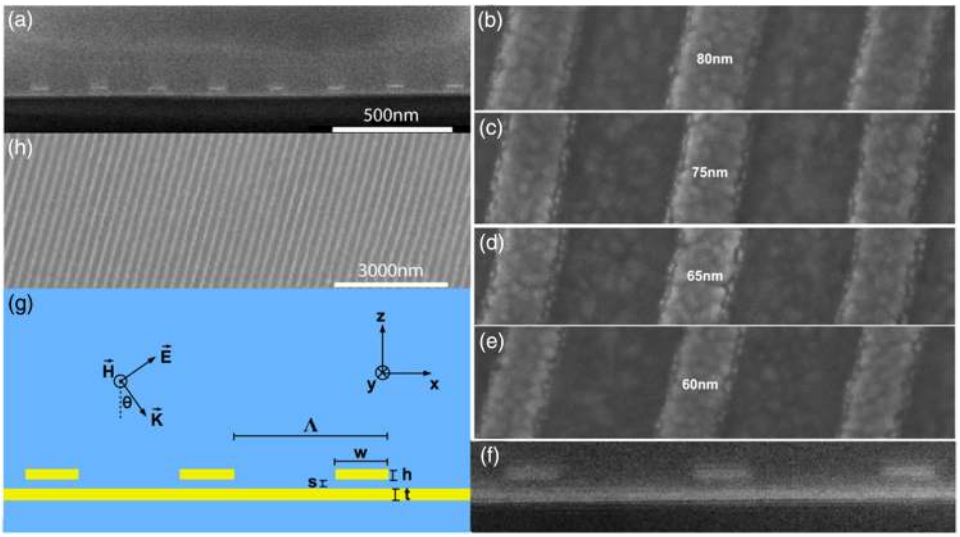

Fig. 1 The geometry being studied, a plasmonic system composed of a periodic Au grating layer above an Au film. (a) SEM image of a cross-sectional cut in the x-z plane. (b) to (e) Tilted SEM top views in the x-y plane showing grating widths of approximately $w = 80$, 75, 65, and 60 nm, respectively. (f) Close-up SEM image of an x-z cross-section. (g) Schematic of the simulated structure with structural parameters $s = 20$ nm, $t = 25$ nm, $w = 80$, 75, 65, and 60 nm, $h = 15$ nm, and $\Lambda = 250$ nm. The structure is embedded in a glass background of permittivity $\varepsilon = 2.13$. (h) Tilted SEM top views in the x-y plane showing the large-scale uniformity of the gratings.

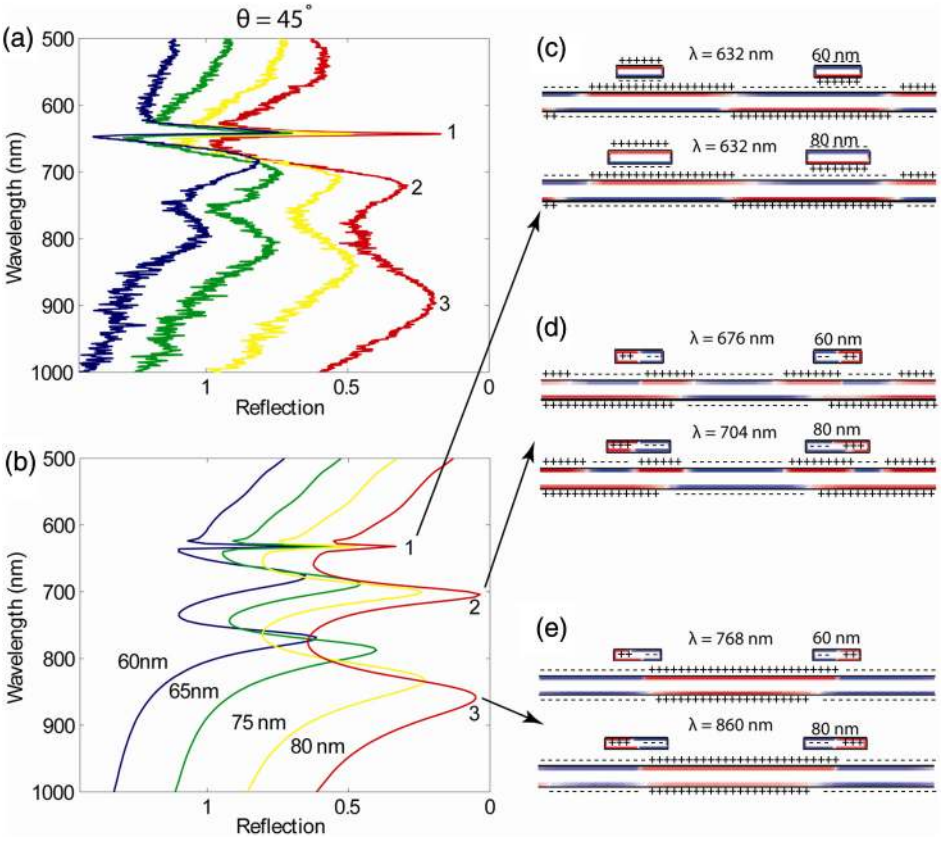

Fig. 2 (a) Measured and (b) simulated reflection spectra at $\theta = 45$ deg incidence for gratings of widths $w = 80$, 75, 65, and 60 nm. Each curve is displaced by an amount of 0.2 from the previous one for viewing purposes. (c) Surface charges for band 1 showing an odd surface plasmon-polariton (SPP) resonance. (d) Surface charges for band 2 showing a parallel hybridization combination of the even/compound SPP and the localized dipole+mirror image resonance. (e) Surface charges for band 3 showing the antiparallel hybridization combination.

varying from $w = 60$ to 80 nm. Note that the 15 nm height of the gratings gives them a somewhat grainy structure; thus, measured widths correspond to the average dimension and exclude grains at the edges. A very good agreement, however, is still seen between experiment and theory in the subsequent figures, thereby demonstrating that the spectral response of the structures is very resilient to fabrication imperfections. Experimental measurements in reflection are made via the same homemade surface plasmon resonance spectrometer described in a previous work,[55] allowing for easy analysis over a wide range of incidence angles and wavelengths. The sample was attached onto the cylindrical prism of the measurement setup from the grating side via index matching gel, thus effectively providing a complete glass background.

2.2 *Theoretical*

Simulations were performed via a surface integral equation method adapted to periodic structures.[56] Thicknesses of the various layers were taken directly from the evaporation parameters and grating widths were taken from the SEM measurements shown in Fig. 1. The dielectric permittivity of Au was taken from experimentally measured data[57] and that of the glass background was set at $\varepsilon = 2.13$.

3 Discussion of Results

In such a system three resonances are expected.[52] The first is a long-range/odd SPP resonance due almost purely to the grating periodicity. The second is a compound resonance based on the

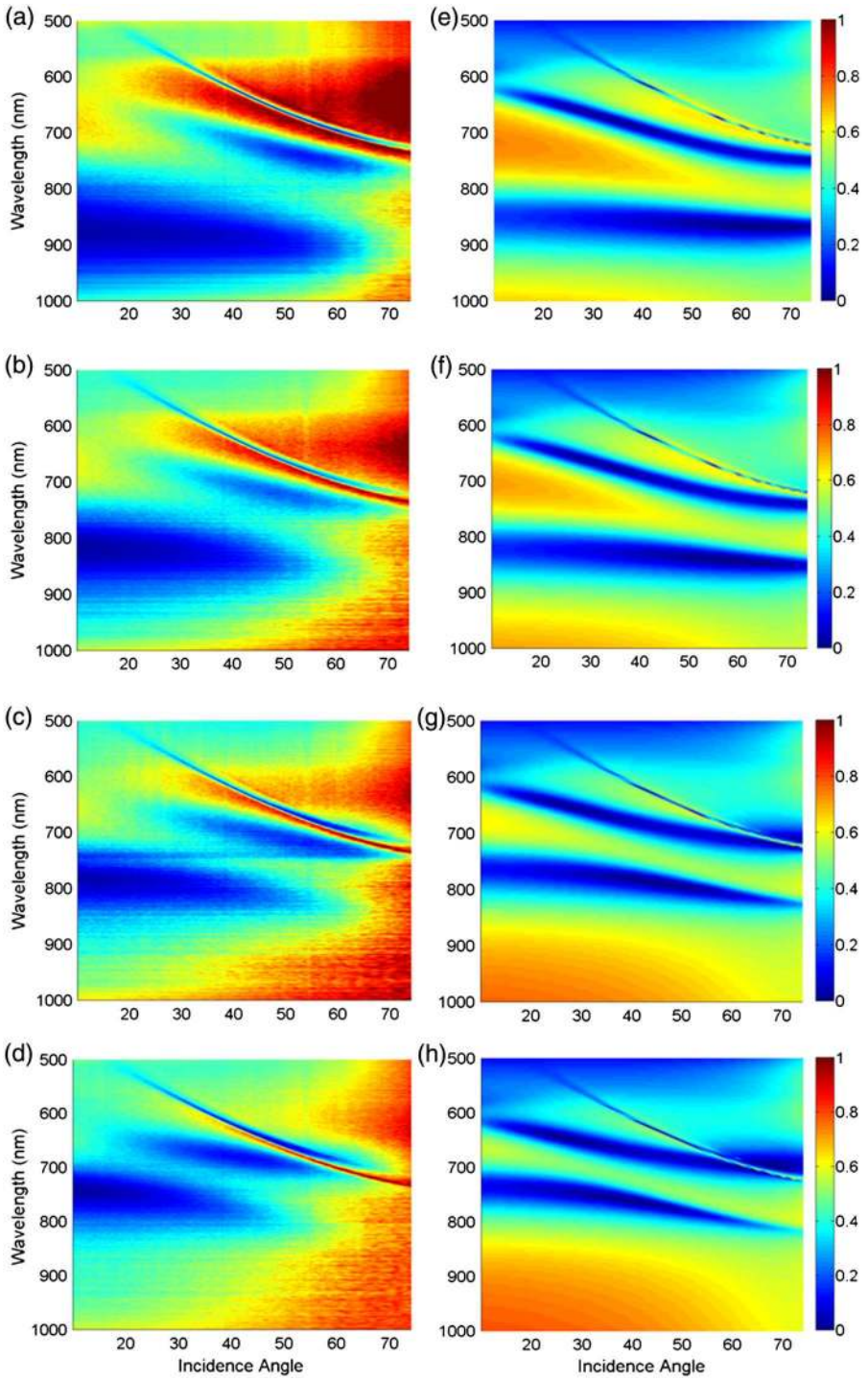

Fig. 3 Reflection spectra of the geometry shown in Fig. 1 for grating widths $w = 80$, 75, 65, and 60 nm, respectively, via [(a) to (d)] experimental measurements and [(e) to (h)] numerical simulations. The leftmost stationary band is that of the grating excited odd SPP resonance, while the remaining two are the parallel and antiparallel hybridization of the even/compound SPP resonance and the localized dipole+mirror image resonance.

short-range/even SPP, whose spectral position varies not only with the structural periodicity, but also with the grating width. This is due to the fact that the charges along the width of the grating elements effectively mirror the charges of the even SPP resonance in the film.[52] The third resonance is that of a dipole resonance in the grating elements coupled to its mirror image in

the underlying film. Its resonance thus varies much more with a change in the grating size. As a consequence, if the widths of the grating elements are reduced sufficiently, this resonance will be greatly blueshifted toward the even/compound SPP resonance and an additional coupling interaction will occur between the two, resulting in a parallel and an antiparallel hybridization combination.[52]

The measured and simulated reflection spectra shown in Figs. 2(a) and 2(b) for $\theta = 45$ deg incidence and gratings of widths 80, 75, 65, and 60 nm exhibit exactly three bands. Additionally, the dispersion of these three bands and their spectral interactions over a large range of incidence angles agree remarkably well with the simulated reflection spectra of Figs. 3(a) to 3(h). The sharpest and most narrowband resonance whose spectral position does not vary with grating size is simply the grating-induced odd (long-range) SPP. This can be verified by plotting the surface charges at the resonance wavelength of $\lambda = 632$ nm for grating widths of both $w = 60$ and 80 nm [Fig. 2(c)]. Indeed, the two cases show surface charges that alternate between positive and negative both along the length of the film and between the top and bottom interfaces, i.e., they exhibit an asymmetric charge distribution characteristic of the long-range SPP.[5] The remaining two bands are that of the even (short-range)/compound SPP resonance and the localized dipolar resonance of the grating elements.[52] For the grating widths studied here, the close spectral proximity of these remaining two has resulted in a parallel and antiparallel hybridization combination with the charge distributions shown in Figs. 2(d) and 2(e). It is easiest to understand this hybridization by first reviewing the response of the system when the two resonances are not hybridized.

When the spectral separation between the two bands is large, such hybridization is not present. In this case, the second band, the even/compound SPP resonance, will exhibit symmetric charges along the two sides of the film, which induce oppositely oriented charges in the grating elements.[52] The third band will simply exhibit a strong localized field and dipolar charge response within the grating elements, which then induces opposite/mirror charges at the top surface of the metallic film.[52] The hybridization of these two will thus result in a combination of the dipolar response within the grating elements and the even SPP of the film. The higher-energy hybridized resonance will be a parallel combination of the dipolar charges in the grating element and the symmetric charge distribution of the even SPP in the film, while the lower-energy one will be an antiparallel combination (Fig. 4). In the antiparallel combination, the dipolar charges in the grating elements are simply out of phase with those of symmetric charge distribution in the metallic film. In the parallel hybridization combination, they begin in phase; however, since localized dipolar charges spaced just nanometers above a metallic film always induce mirror charges in the top surface of the film, one will obtain the charge distribution illustrated in Fig. 4. Here the induced charges along the top interface of the film that lie directly below the grating elements are effectively reversed from those along the bottom interface of the film.

This hybridization can clearly be observed by viewing not only the surface charges of the two at resonance [Figs. 2(d) and 2(e)], but also the spectral interaction of the two bands in Figs. 3(a) to 3(h). In all of these plots, a clear anti-crossing is seen, specifically at higher incidence angles,

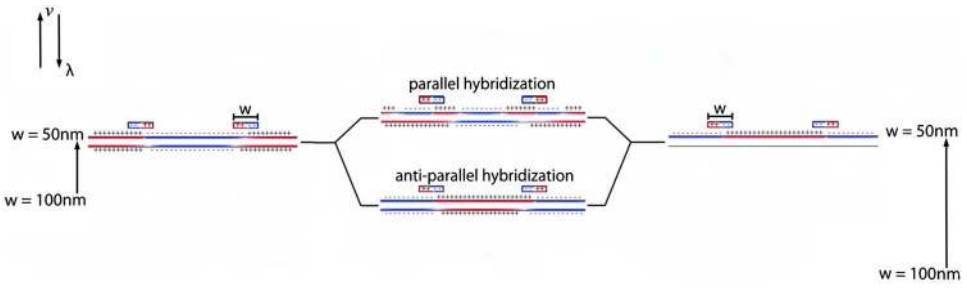

Fig. 4 Hybridization diagram of the even/compound SPP resonance and the localized dipole+mirror image resonance. As the width w of the grating elements is reduced, a slight blueshift of one resonance and a much larger blueshift of the other resonance places the two at the same frequency, thus resulting in a coupling interaction, which in turn gives rise to a parallel and antiparallel hybridization combination.

where the normally nondispersive localized dipole+mirror image resonance is redshifted due to a spectral overlap with the even/compound SPP resonance. Furthermore, it can clearly be deduced that for gratings of much larger widths, the hybridization of the two resonances will cease, and the system will tend back to that of two unhybridized resonances, the first being the even/compound SPP resonance and the second the localized dipole+mirror image resonance.[52]

4 Conclusions

In conclusion, we have fabricated a large-area plasmonic grating with sub-100 nm features on film structures via EUV-IL that support propagation of not only plasmon resonances, but also hybridized compound plasmonic resonances. Experimentally measured reflection spectra over a wide range of incidence angles and excitation wavelengths show the existence of these resonances and their spectral evolution with varying grating size. These experimental findings are confirmed with both numerically calculated reflection spectra—which show an excellent agreement—and surface charge plots, thus revealing the underlying mechanisms associated with each mode. These large-scale fabricated compound plasmonic structures exhibit highly versatile tunability, enhanced optical properties, and resiliency to possible fabrication imperfections. We expect the simplicity in the fabrication of these structures, specifically on a large scale, to be extendable to more complex multilayered structures exhibiting three-dimensional optical metamaterial properties.

Acknowledgments

Funding from the State Secretariat for Education and Research within the Indo Swiss Joint Research Programme and from the Swiss National Science Foundation (projects 200021-125326 and 200021-124777) is gratefully acknowledged. Part of this work was performed at the Swiss Light Source, Paul Scherrer Institute in Switzerland, where Thomas Siegfried and Dr. Yasin Ekinci fabricated the grating on film structures under the supervision of Dr. Hans Sigg.

References

1. E. Kretschmann and H. Raether, "Radiative decay of non-radiative surface plasmons excited by light," *Z. Naturforsch. A* **23**, 2135 (1968).
2. A. Otto, "Excitation of nonradiative surface plasma waves in silver by the method of frustrated total reflection," *Z. Phys.* **216**(4), 398 (1968), http://dx.doi.org/10.1007/BF01391532.
3. W. L. Barnes, A. Dereux, and T. W. Ebbesen, "Surface plasmon subwavelength optics," *Nature* **424**(6950), 824–830 (2003), http://dx.doi.org/10.1038/nature01937.
4. H. Raether, "Surface plasmons on smooth and rough surfaces and on gratings," *Springer Tracts Mod. Phys.* **111**, 1–133 (1988), http://dx.doi.org/10.1007/BFb0048317.
5. P. Berini, "Long-range surface plasmon polaritons," *Adv. Opt. Photon.* **1**(3), 484–588 (2009), http://dx.doi.org/10.1364/AOP.1.000484.
6. W. Zhang et al., "Trapping and sensing 10 nm metal nanoparticles using plasmonic dipole antennas," *Nano Lett.* **10**(3), 1006–1011 (2010), http://dx.doi.org/10.1021/nl904168f.
7. A. Lovera and O. J. F. Martin, "Plasmonic trapping with realistic dipole nanoantennas: analysis of the detection limit," *Appl. Phys. Lett.* **99**(15), 151104 (2011), http://dx.doi.org/10.1063/1.3650267.
8. L. R. Hirsch et al., "Nanoshell-mediated near-infrared thermal therapy of tumors under magnetic resonance guidance," *Proc. Natl. Acad. Sci. U. S. A.* **100**(23), 13549–13554 (2003), http://dx.doi.org/10.1073/pnas.2232479100.
9. D. P. O'Neal et al., "Photo-thermal tumor ablation in mice using near infrared-absorbing nanoparticles," *Cancer Lett.* **209**(2), 171–176 (2004), http://dx.doi.org/10.1016/j.canlet.2004.02.004.
10. J. Chen et al., "Immuno gold nanocages with tailored optical properties for targeted photothermal destruction of cancer cells," *Nano Lett.* **7**(5), 1318–1322 (2007), http://dx.doi.org/10.1021/nl070345g.

11. A. M. Gobin et al., "Near-infrared resonant nanoshells for combined optical imaging and photothermal cancer therapy," *Nano Lett.* **7**(7), 1929–1934 (2007), http://dx.doi.org/10.1021/nl070610y.
12. X. Qian et al., "In vivo tumor targeting and spectroscopic detection with surface-enhanced Raman nanoparticle tags," *Nat. Biotechnol.* **26**(1), 83–90 (2007), http://dx.doi.org/10.1038/nbt1377.
13. W. Zhang et al., "Mode-selective surface-enhanced Raman spectroscopy using nanofabricated plasmonic dipole antennas," *J. Phys. Chem. C* **113**(33), 14672–14675 (2009), http://dx.doi.org/10.1021/jp9042304.
14. A. M. Kern, A. J. Meixner, and O. J. F. Martin, "Molecule-dependent plasmonic enhancement of fluorescence and Raman scattering near realistic nanostructures," *ACS Nano* **6**(11), 9828–9836 (2012), http://dx.doi.org/10.1021/nn3033612.
15. T. Siegfried et al., "Reusable plasmonic substrates fabricated by interference lithography: a platform for systematic sensing studies," *J. Raman Spectrosc.* **44**(2), 170–175 (2013), http://dx.doi.org/10.1002/jrs.v44.2.
16. K. R. Catchpole and A. Polman, "Plasmonic solar cells," *Opt. Express* **16**(26), 21793–21800 (2008), http://dx.doi.org/10.1364/OE.16.021793.
17. Y. A. Akimov and W. S. Koh, "Design of plasmonic nanoparticles for efficient subwavelength light trapping in thin-film solar cells," *Plasmonics* **6**(1), 155–161 (2011), http://dx.doi.org/10.1007/s11468-010-9181-4.
18. J. Homola, Ed., *Surface Plasmon Resonance Based Sensors*, Springer, Berlin, Heidelberg, New York (2006).
19. M. Piliarik, L. Parova, and J. Homola, "High-throughput SPR sensor for food safety," *Biosens. Bioelectron.* **24**(5), 1399–1404 (2009), http://dx.doi.org/10.1016/j.bios.2008.08.012.
20. J. A. Conway, S. Sahni, and T. Szkopek, "Plasmonic interconnects versus conventional interconnects: a comparison of latency, crosstalk and energy costs," *Opt. Express* **15**(8), 4474–4484 (2007), http://dx.doi.org/10.1364/OE.15.004474.
21. J. J. Ju et al., "40 gbit/s light signal transmission in long-range surface plasmon waveguides," *Appl. Phys. Lett.* **91**(17), 171117 (2007), http://dx.doi.org/10.1063/1.2803069.
22. J. T. Kim et al., "Chip-to-chip optical interconnect using gold long-range surface plasmon polariton waveguides," *Opt. Express* **16**(17), 13133–13138 (2008), http://dx.doi.org/10.1364/OE.16.013133.
23. S. Park et al., "Long range surface plasmon polariton waveguides at 1.31 and 1.55 um wavelengths," *Opt. Commun.* **281**(8), 2057–2061 (2008), http://dx.doi.org/10.1016/j.optcom.2007.10.115.
24. W. R. Holland and D. G. Hall, "Surface-plasmon dispersion relation: shifts induced by the interaction with localized plasma resonances," *Phys. Rev. B* **27**, 7765 (1983), http://dx.doi.org/10.1103/PhysRevB.27.7765.
25. P. Nordlander and E. Prodan, "Plasmon hybridization in nanoparticles near metallic surfaces," *Nano Lett.* **4**(11), 2209–2213 (2004), http://dx.doi.org/10.1021/nl0486160.
26. J. Cesario et al., "Electromagnetic coupling between a metal nanoparticle grating and a metallic surface," *Opt. Lett.* **30**(24), 3404–3406 (2005), http://dx.doi.org/10.1364/OL.30.003404.
27. G. Lévêque and O. J. F. Martin, "Optical interactions in a plasmonic particle coupled to a metallic film," *Opt. Express* **14**(21), 9971–9981 (2006), http://dx.doi.org/10.1364/OE.14.009971.
28. G. Lévêque and O. J. F. Martin, "Tunable composite nanoparticle for plasmonics," *Opt. Lett.* **31**(18), 2750–2752 (2006), http://dx.doi.org/10.1364/OL.31.002750.
29. N. Papanikolaou, "Optical properties of metallic nanoparticle arrays on a thin metallic film," *Phys. Rev. B* **75**(23), 235426 (2007), http://dx.doi.org/10.1103/PhysRevB.75.235426.
30. F. Le et al., "Plasmonic interactions between a metallic nanoshell and a thin metallic film," *Phys. Rev. B* **76**(16), 165410 (2007), http://dx.doi.org/10.1103/PhysRevB.76.165410.
31. N. Liu et al., "Plasmon hybridization in stacked cut-wire metamaterials," *Adv. Mater.* **19**(21), 3628–3632 (2007), http://dx.doi.org/10.1002/(ISSN)1521-4095.

32. J. J. Mock et al., "Distance-dependent plasmon resonant coupling between a gold nanoparticle and gold film," *Nano Lett.* **8**(8), 2245–2252 (2008), http://dx.doi.org/10.1021/nl080872f.
33. S. Malynych and G. Chumanov, "Narrow plasmon mode in 2d arrays of silver nanoparticles self-assembled on thin silver films," *J. Microsc.* **229**(3), 567–574 (2008), http://dx.doi.org/10.1111/j.1365-2818.2008.01945.x.
34. A. Christ et al., "Near-field-induced tunability of surface plasmon polaritons in composite metallic nanostructures," *J. Microsc.* **229**(2), 344–353 (2008), http://dx.doi.org/10.1111/j.1365-2818.2008.01911.x.
35. G. Lévêque and R. Quidant, "Channeling light along a chain of near-field coupled gold nanoparticles near a metallic film," *Opt. Express* **16**(26), 22029–22038 (2008), http://dx.doi.org/10.1364/OE.16.022029.
36. G. Lévêque and O. J. F. Martin, "Narrow-band multiresonant plasmon nanostructure for the coherent control of light: an optical analog of the xylophone," *Phys. Rev. Lett.* **100**(11), 117402 (2008), http://dx.doi.org/10.1103/PhysRevLett.100.117402.
37. D. Brunazzo, E. Descrovi, and O. J. F. Martin, "Narrowband optical interactions in a plasmonic nanoparticle chain coupled to a metallic film," *Opt. Lett.* **34**(9), 1405–1407 (2009), http://dx.doi.org/10.1364/OL.34.001405.
38. Y. Chu and K. B. Crozier, "Experimental study of the interaction between localized and propagating surface plasmons," *Opt. Lett.* **34**(3), 244–246 (2009), http://dx.doi.org/10.1364/OL.34.000244.
39. A. Ghoshal, I. Divliansky, and P. G. Kik, "Experimental observation of mode-selective anticrossing in surface-plasmon-coupled metal nanoparticle arrays," *Appl. Phys. Lett.* **94**(17), 171108 (2009), http://dx.doi.org/10.1063/1.3122922.
40. K. Wang, E. Schonbrun, and K. B. Crozier, "Propulsion of gold nanoparticles with surface plasmon polaritons: evidence of enhanced optical force from near-field coupling between gold particle and gold film," *Nano Lett.* **9**(7), 2623–2629 (2009), http://dx.doi.org/10.1021/nl900944y.
41. N. Liu and H. Giessen, "Coupling effects in optical metamaterials," *Angew. Chem. Int. Ed.* **49**(51), 9838–9852 (2010), http://dx.doi.org/10.1002/anie.v49.51.
42. J. DiMaria and R. Paiella, "Plasmonic dispersion engineering of coupled metal nanoparticle-film systems," *J. Appl. Phys.* **111**(10), 103102 (2012), http://dx.doi.org/10.1063/1.4717763.
43. A. Farhang, A. Ramakrishna, and O. J. F. Martin, "Multipolar effects and strong coupling in hybrid plasmonic metamaterials," *Proc. SPIE* **8269**, 82691B (2012), http://dx.doi.org/10.1117/12.908923.
44. C. Wang et al., "Role of mode coupling on transmission properties of subwavelength composite hole-patch structures," *Appl. Phys. Lett.* **96**(25), 251102 (2010), http://dx.doi.org/10.1063/1.3456377.
45. J. Cesario et al., "Coupling localized and extended plasmons to improve the light extraction through metal films," *Opt. Express* **15**(17), 10533–10539 (2007), http://dx.doi.org/10.1364/OE.15.010533.
46. J. Hao et al., "High performance optical absorber based on a plasmonic metamaterial," *Appl. Phys. Lett.* **96**(25), 251104 (2010), http://dx.doi.org/10.1063/1.3442904.
47. C. Koechlin et al., "Total routing and absorption of photons in dual color plasmonic antennas," *Appl. Phys. Lett.* **99**(24), 241104 (2011), http://dx.doi.org/10.1063/1.3670051.
48. K. Aydin et al., "Broadband polarization-independent resonant light absorption using ultrathin plasmonic super absorbers," *Nat. Commun.* **2**, 517 (2011), http://dx.doi.org/10.1038/ncomms1528.
49. Y. Cui et al., "Ultrabroadband light absorption by a sawtooth anisotropic metamaterial slab," *Nano Lett.* **12**(3), 1443–1447 (2012), http://dx.doi.org/10.1021/nl204118h.
50. J. Wang et al., "Tunable broad-band perfect absorber by exciting of multiple plasmon resonances at optical frequency," *Opt. Express* **20**(14), 14871–14878 (2012), http://dx.doi.org/10.1364/OE.20.014871.
51. T. J. Seok et al., "Radiation engineering of optical antennas for maximum field enhancement," *Nano Lett.* **11**(7), 2606–2610 (2011), http://dx.doi.org/10.1021/nl2010862.

52. A. Farhang, S. A. Ramakrishna, and O. J. F. Martin, "Compound resonance-induced coupling effects in composite plasmonic metamaterials," *Opt. Express* **20**(28), 29447–29456 (2012), http://dx.doi.org/10.1364/OE.20.029447.
53. T. Siegfried et al., "Engineering metal adhesion layers that do not deteriorate plasmon resonances," *ACS Nano* **7**(3), 2751–2757 (2013), http://dx.doi.org/10.1021/nn4002006.
54. V. Auzelyte et al., "Extreme ultraviolet interference lithography at the Paul Scherrer Institute," *J. Micro Nanolithogr. MEMS MOEMS* **8**(2), 021204 (2009), http://dx.doi.org/10.1117/1.3116559.
55. A. Farhang et al., "Broadband wide-angle dispersion measurements: instrumental setup, alignment, and pitfalls," *Rev. Sci. Instrum.* **84**(3), 033107 (2013), http://dx.doi.org/10.1063/1.4795455.
56. B. Gallinet, A. M. Kern, and O. J. F. Martin, "Accurate and versatile modeling of electromagnetic scattering on periodic nanostructures with a surface integral approach," *J. Opt. Soc. Am. A* **27**(10), 2261–2271 (2010), http://dx.doi.org/10.1364/JOSAA.27.002261.
57. P. B. Johnson and R. W. Christy, "Optical constants of the nobel metals," *Phys. Rev. B* **6**(12), 4370–4379 (1972), http://dx.doi.org/10.1103/PhysRevB.6.4370.

Arash Farhang received his bachelor's degree in electrical engineering from the University of Utah, where he studied from 2005 to 2009. Since December of 2009, he has been doing his PhD studies in plasmonics at the Nanophtonics and Metrology Lab at the Swiss Federal Institute of Technology, Lausanne, Switzerland. The goal of his work is to explore compound plasmonic systems, which support both localized and delocalized/propagating plasmon modes.

Thomas Siegfried received his graduate diploma in chemical- and bioengineering from Friedrich Alexander University, Germany, in 2009. He currently pursues his PhD work on periodic arrays for plasmonic substrates at the Laboratory for Micro- and Nanotechnology, Paul Scherrer Institute in Switzerland. His research interest covers large area patterning, sub-10 nm gap arrays, surface-enhanced Raman, fluorescence and nonlinear spectroscopy, surface functionalization, and finite-element simulations.

Yasin Ekinci received his PhD from Max Planck Institute in Göttingen, Germany, in 2003. He worked at Paul Scherrer Institute and at the Swiss Federal Institute of Technology, Zurich, Switzerland. Since 2009, he is a senior scientist at Paul Scherrer Institute. He is the manager of the XIL-II beamline at Swiss Light Source. He leads the nanooptics group in the Laboratory for Micro- and Nanotechnology, where he works on EUV interference lithography and nanooptics.

Hans Sigg received his PhD in physics from the Katholieke University Nijmegen of the Netherlands in 1985 for his work on magneto-spectroscopy of semiconductors. After four years postdoc at the Max Planck Institute in Stuttgart, working on the optical properties of two-dimensional electron systems in Klaus von Klitzing's research group, he was hired as a staff scientist by the Paul Scherrer Institute in 1990. Current research interests include mesoscopic effects in semiconductors, Si photonics, and plasmonics in the visible and infrared.

Olivier J. F. Martin received his MSc and PhD degrees in physics from the Swiss Federal Institute of Technology, Lausanne (EPFL), Switzerland. In 1989, he joined IBM Zurich Research Laboratory, where he investigated thermal and optical properties of semiconductor laser diodes. He is currently full professor for nanophotonics and optical signal processing at EPFL, where he is director of the Nanophotonics and Metrology Laboratory and conducts research in plasmonics.